Phase diagram for the trapped p-wave fermionic superfluid with population imbalance

Ammar Kirmani, Khandker Quader, and Maxim Dzero
Department of Physics, Kent State University, Kent, Ohio 44240, USA
(Received 1 January 2017; published 6 April 2017)

We consider the problem of spin-triplet p-wave superfluid pairing with total spin projection $m_s = 0$ in atomic Fermi gas across the Feshbach resonance. We allow for imbalanced populations and take into account the effects due to the presence of a harmonic trapping potential. Within the mean-field approximation for the one- and two-channel pairing models we show that the p-wave superfluid state has the lowest energy up to some distance from the trap center, the distance depending on population imbalance and the side of the Feshbach resonance (BCS or BEC) the system is in. Beyond this, the system is in the normal state. Since the system, even in the presence of the harmonic trap, is invariant under O(3) space rotation, the superfluid cores which emerge in the trap are comprised of states that are degenerate with respect to the "orbital ferromagnet" state, $p_x \pm ip_y$, as well as the ones in which all angular momentum components of the order parameter are nonzero, provided the modulus of the order parameter maintains a fixed magnitude.

DOI: 10.1103/PhysRevB.95.134503

I. INTRODUCTION

The experimental discovery of the p-wave Feshbach resonance (FR) [1–5] in ultracold fermions has led to a flurry of theoretical work addressing various aspects of the superfluid pairing across the BCS-BEC crossover where the single fermionic atoms are adiabatically converted to the diatomic molecules as one varies the resonance detuning frequency [6]. Notably, interest in the physics of the p-wave FR in two-dimensional condensates has been rekindled due to the possibility of the topological phase transition [7,8] as well as its realization as the system is driven out of equilibrium [9,10]. Cold fermion systems with unequally populated hyperfine states, and/or unequal mass, as in mixtures [11], provide an avenue for exploration of potentially rich physics. These may also be relevant to other systems with unequal population, such as in quark matter [12] and magnetic field induced superconductors [13]. Past theory work on p-wave pairing for unequal population has been limited especially in the presence of a trap [14].

In realistic experimental situations, however, the condensate is subject to either external optical trapping potential or to an underlying optical lattice. For the case of the s-wave pairing it has been shown that the presence of the optical trap together with the mass and population imbalance leads to a variety of the superfluid states some of which are of exotic nature, such as a breached pairing state, for example [15–17].

In general, spin triplet ($s = 1, m_s = 0, \pm 1$) p-wave fermion pairing with orbital quantum number $m = 0, \pm 1$ can give rise to a rich variety of superfluid ground states, some of which are realized in superfluid phases of liquid ^{3}He. However, for a given system, absent additional symmetry and physical constraints, a general consideration can be daunting, even when restricted to unitary cases. As it has been discussed in Refs. [18,19], considerable simplification is afforded by cold atoms subject to p-wave FR: Different for liquid ^{3}He, pairing interaction may be highly anisotropic in "spin" space ("spin" referring to hyperfine states). For example, in ^{6}Li, when the hyperfine pair $|m_s, m_s'\rangle = |1/2, -1/2\rangle$ is at resonance, the pairs $|1/2, 1/2\rangle$ and $|-1/2, -1/2\rangle$ may not be. Pairs in p-wave superfluids with unequal "spin" components can however have different $l = 1$ components, namely $m = 0, \pm 1$. Consequently, the components of the pairing wave function Δ_{lm} are related to the spherical harmonics $Y_l^m(\theta, \varphi)$.

In the context of cold atoms, spin triplet p-wave superfluidity with $m_s = 0$ has been studied at the mean-field level, for equal population in Ref. [18] and for arbitrary population imbalance in Ref. [19], but in both cases without trapping potential. In Ref. [18], the ground state was found to be an "orbital ferromagnet", $p_x \pm ip_y$, in which either $\Delta_{1,1}$ or $\Delta_{1,-1}$ pairing gap component is nonzero. On the other hand, in keeping with the rotational O(3) symmetry of the system with isotropic interaction, Ref. [19] found the ground state to be degenerate with respect to the state $p_x \pm ip_y$, and the ones in which all angular momentum components of the order parameter are nonzero. Additionally, this work suggested that, across the FR, the states which have higher energy for zero population imbalance, e.g. the "polar" state, $\Delta_{1,0}$, may acquire a lower energy for nonzero population imbalance, P, thereby becoming the ground state, provided P exceeded some critical value.

There are several motivations for considering p-wave superfluidity of cold fermions in a trap. First, to the best of our knowledge the problem of the $m_s = 0$ spin triplet p-wave pairing with nonzero trapping potential has never been addressed and we attempt to fill this gap in this paper. Next, owing to the trap potential, the chemical potential is spatially dependent via a local density approximation (LDA); this is expected to lead to spatially dependent ground-state phases, which can have interesting consequences. Then, since we are considering arbitrary "spin" population imbalance, we anticipate rich physics to emerge from the interplay between the population imbalance and the presence of the trap; our goal is to map out the behavior of the system in the space of population imbalance and trap potential. For example, while the breached pair (BP) states do arise in population imbalanced p-wave superfluid calculations, even in the absence of a trap [20], breached pair state of one particular type, namely BP1 (explored and explained later) is expected to arise more naturally in calculations here, owing to the finite-range interaction (necessary for realizing a p-wave state)

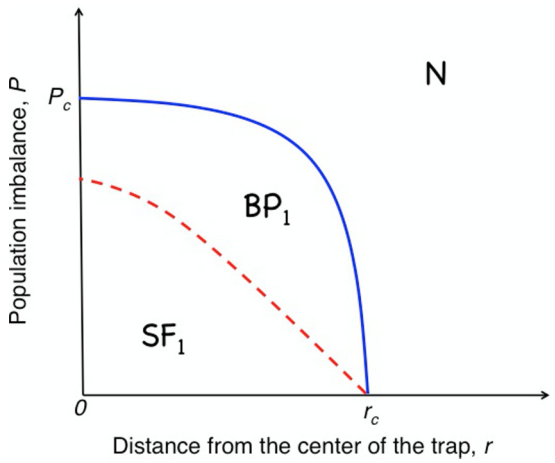

FIG. 1. Schematic phase diagram for the $m_s = 0$ p-wave superfluid subject to harmonic potential. State SF_1 denotes a doubly degenerate superfluid state which breaks time-reversal symmetry. The energy of SF_1 equals to the energy of TRI superfluid state SF_0 corresponding to the state when all angular momentum components of the pairing wave function are nonzero. The dashed line separates the SF_1 state with the superfluid breached pairing state BP_1 in which parts of the Fermi surface remain unpaired supporting the gapless excitations. Parameters r_c and P_c denote the positions in the trap and value of the population imbalance for which the first-order transition between superfluid and normal state takes place.

and its interplay with the spatially-dependent trap potential. Also, since any likely experiment will be carried out in a trap, calculations of properties of a p-wave superfluid for a population imbalanced system in a harmonic trap would provide a more direct comparison to experiments.

Accordingly, we consider the pairing problem within the one- and two-channel p-wave pairing models and explore the effects of harmonic (anisotropic in general) trapping potential by adopting the local density approximation (LDA). We utilize the mean-field theory approach to compute the ground state energy across the FR as a function of the distance from the center of the trap, r, and at the same time allow for arbitrary population imbalance. Our main results can be summarized on a schematic phase diagram in the (r, P) plane, Fig. 1. If we are constrained to the center of the trap, $r = 0$, and start increasing the population imbalance than there is a phase transition between the superfluid (SF_1) and the normal (N) state and, in addition, within the superfluid state there exists a breached pairing state (BP_1) in which single fermionic excitations become gapless for some values of momenta. Parabolic trapping potential leads to qualitatively the same physics: As the distance from the center of the trap increases the phase transition between two different superfluid states—SF_1 and the breached pairing state BP_1—takes place. Note, that both r_c and P_c are not universal and depend on the detuning frequency. For example, we find that the region of the trap where the BP_1 is realized gets wider as one goes from the BCS to the BEC side of the FR resonance.

The remaining part of the paper is organized as follows. In Sec. II, we present the two-channel model, basic equations, and approximations we use to study the $m_s = 0$ triplet p-wave superfluid in a parabolic trap. We also present a Ginzburg-Landau analysis which we later use as a guide to obtain solutions of the mean-field self-consistency equations. In Sec. III we present and discuss our main results for the two-channel model. We also present results and discussions of the single-channel model, relevant for wide resonances in Sec. IV. Section V contains concluding discussion followed by acknowledgments. Lastly, in the appendix we provide detailed analysis of the self-consistency equations which guide the search for the system's ground state energy as a function of the distance from the center of the trap.

II. TWO-CHANNEL MODEL AND BASIC EQUATIONS

We present a two-channel model which describes fermionic atoms in two hyperfine states interacting via p-wave $m_s = 0$ triplet Feshbach resonance. We consider systems with arbitrary population imbalances. In our two-channel model molecules with nonzero center-of-mass momenta are ignored. With this provision the model Hamiltonian reads

$$H = \sum_{\mathbf{k}\sigma} \epsilon_{\mathbf{k}\sigma} \hat{c}^\dagger_{\mathbf{k}\sigma} \hat{c}_{\mathbf{k}\sigma} + \omega \sum_{m=-1}^{1} \hat{b}^\dagger_m \hat{b}_m + g \sum_{\mathbf{k}} \sum_{m=-1}^{1} w_{\mathbf{k}} [Y_{1m}(\hat{\mathbf{k}}) \hat{b}_m \hat{c}^\dagger_{\mathbf{k}\uparrow} \hat{c}^\dagger_{-\mathbf{k}\downarrow} + \text{H.c.}]. \quad (2.1)$$

Here g is a coupling constant, $\hat{c}^\dagger_{\mathbf{k}\sigma}, \hat{c}_{\mathbf{k}\sigma}$ are fermionic creation and annihilation operators, $\sigma = \uparrow, \downarrow$ denotes the two hyperfine states, and $\epsilon_{\mathbf{k}\sigma}$ are single particle energies given by

$$\epsilon_{\mathbf{k}\sigma} = \frac{k^2}{2m} - h \cdot \text{sgn}(\sigma); \quad (2.2)$$

$\hat{b}^\dagger_m$, $\hat{b}_m$ are the bosonic operators which describe the creation and annihilation of molecules with the orbital quantum number $m = 0, \pm 1$ of binding energy ω. The parameter h accounts for the population imbalance between the two hyperfine states. Equation (2.1) is obtained assuming a separable from the two-body fermion interaction: $V_{k,k'} = g w_k w_{k'}$. The separable form is chosen for convenience [18,21,22] and does not qualitatively change the physics. For w_k, we have chosen the Nozieres-Schmitt-Rink form [22]: $w_{\mathbf{k}} = k_0 k/(k^2 + k_0^2)$ with $k_0 \sim k_F$ guarantees the convergence of the momenta summations, so that one does not need to introduce the ultraviolet cutoff. Just as in the case of an s-wave condensate, the model (2.1) describes superfluid fermions—BCS side of the Feshbach resonance—when ω exceeds the Fermi energy ε_F and bound molecules when ω is decreased below the Fermi energy, so that deep in the BEC regime $\omega < 0$ and $|\omega| \gg \varepsilon_F$.

In the mean-field approximation, the bosonic operators in the Hamiltonian (2.1) are replaced with their expectation values, $\hat{b}_m \to b_m = \langle \hat{b}_m \rangle$. In what follows, it will be convenient to introduce the pairing fields

$$\Delta_m = -g b_m. \quad (2.3)$$

In complete analogy with the discussion on the mean-field theory for the two-channel s-wave model in Ref. [23], we obtain the following zero-temperature self-consistency

equations for the pairing field components

$$\Delta_m = \frac{g^2}{(\omega - 2\mu)} \sum_{\mathbf{k}} \frac{w_k^2 \theta(E_{\mathbf{k}} - h)}{2\sqrt{\xi_{\mathbf{k}}^2 + |\Delta(\mathbf{k})|^2}} \times \sum_{n=-1}^{1} Y_{1m}^*(\hat{\mathbf{k}}) Y_{1n}(\hat{\mathbf{k}}) \Delta_n, \tag{2.4}$$

where $\xi_{\mathbf{k}} = k^2/2m - \mu$, $E_{\mathbf{k}} = \sqrt{\xi_{\mathbf{k}}^2 + |\Delta(\mathbf{k})|^2}$, superfluid order parameter $\Delta(\mathbf{k}) = w_k \sum_m Y_{1m}(\hat{\mathbf{k}})\Delta_m$, and μ is the chemical potential determined from the particle number equation

$$2n = \frac{2}{g^2} \sum_{m=-1}^{1} |\Delta_m|^2 + \sum_{\mathbf{k}} \left[1 - \frac{\xi_{\mathbf{k}}}{E_{\mathbf{k}}} \theta(E_{\mathbf{k}} - h) \right], \tag{2.5}$$

where $n = (n_\uparrow + n_\downarrow)/2$ is a total particle density. In Appendix A we provide the detailed analysis of the possible roots of Eqs. (2.4) which will help us with the analysis of the case of the nonzero trapping potential.

In analogy with the s-wave case [6,23], we introduce the dimensionless parameter

$$\gamma = \frac{g^2 \nu_F}{\varepsilon_F} \tag{2.6}$$

and ν_F is the density of states at the Fermi level. This parameter describes the width of the Feshbach resonance and has a physical meaning of the dimensionless interaction strength between the atoms and molecules. For broad Feshbach resonance, $\gamma \gg 1$, the singlet p-wave pairing problem can be addressed in terms of the following single-channel model [18,19]:

$$H_{1\mathrm{ch}} = \sum_{\mathbf{k}\sigma} \xi_{\mathbf{k}\sigma} \bar{c}_{\mathbf{k}\sigma} c_{\mathbf{k}\sigma} - \sum_{\mathbf{kp}} V_{\mathbf{kp}} \bar{c}_{\mathbf{k}\uparrow} \bar{c}_{-\mathbf{k}\downarrow} c_{-\mathbf{p}\downarrow} c_{\mathbf{p}\uparrow}, \tag{2.7}$$

where $V_{\mathbf{kp}} = (\lambda/\nu_F) w_{\mathbf{k}} w_{\mathbf{p}} \sum_{mn} Y_{1m}^*(\hat{\mathbf{k}}) Y_{1n}(\hat{\mathbf{p}})$ and $\lambda > 0$ is the dimensionless pairing strength. It is important to note that while the mean-field approximation for the model (2.7) holds deep in the BEC regime corresponding to $\lambda \gg 1$ as well as in the BCS regime $\lambda \ll 1$, it is not applicable for the intermediate values of the coupling constant, $\lambda \sim 1$. That is why in this paper we will focus more on the physics governed by the two-channel model (2.1), though we also present our results for the one-channel model in Sec. IV.

A. Ginzburg-Landau expansion

To get insight into the energy structure of the p-wave pairing state, it will be useful to utilize the Ginzburg-Landau approach ignoring the trapping potential. At temperatures just below the critical temperature $|T - T_c|/T_c \ll 1$ all order parameter components are small and we can expand the right hand side of the self-consistency equation in powers of $\Delta_m = |\Delta_m| e^{i\phi_m}$ ($m = 0, \pm 1$). The free energy which corresponds to this expansion has the following form

$$\mathcal{F}[\Delta] = \mathcal{F}_0 - a(h,T) \sum_{m=-1}^{1} |\Delta_m|^2 + b(h,T) \sum_{kl} \sum_{mn} \mathcal{I}_{mn}^{kl} \Delta_m^* \Delta_n^* \Delta_k \Delta_l, \tag{2.8}$$

where $\mathcal{F}_0$ is the free energy in the normal state, and the expansion coefficients $a(h,T) > 0$ and $b(h,T) > 0$ are some known functions of the population imbalance and temperature. Using the symmetry of the fourth term with respect to permutations $m \leftrightarrow n$ and $k \leftrightarrow l$, we can compactly rewrite the expression for the coefficients $\mathcal{I}_{mn}^{kl}$ as follows

$$\begin{aligned} \mathcal{I}_{mn}^{kl} = & -2[\delta_{m,0}\delta_{n,0}\delta_{k,-1}\delta_{l,1} + \delta_{m,-1}\delta_{n,1}\delta_{k,0}\delta_{l,0}] \\ & + 4[\delta_{m,-1}\delta_{n,0}\delta_{k,-1}\delta_{l,0} + \delta_{m0}\delta_{n,1}\delta_{k,1}\delta_{l,0}] \\ & + 2[\delta_{m,-1}\delta_{n,-1}\delta_{k,-1}\delta_{l,-1} + \delta_{m,1}\delta_{n,1}\delta_{k,1}\delta_{l,1} \\ & + 4\delta_{m,-1}\delta_{n,1}\delta_{k,1}\delta_{l,-1}] + 3\delta_{m,0}\delta_{n,0}\delta_{k,0}\delta_{l,0}. \end{aligned}$$

A quick analysis of the free energy (2.8) shows that the conditions for the minima of the free energy are satisfied for

$$2\phi_0 - \phi_1 - \phi_{-1} = 2\pi n, \quad (n = 0,1,2,...). \tag{2.9}$$

Let us introduce the following three-component vector $\vec{\Delta} = (|\Delta_{-1}|, \Delta_0, |\Delta_1|)$ and we take into account that Δ_0 can be considered purely real due to condition (2.9). The free energy has a minimum $\mathcal{F}_{\min} = -50a^2/9b$ corresponding to two superfluid states which differ from each other by symmetry. One of these two states denoted by SF_0 is described by $\vec{\Delta}$ with all nonzero components which satisfy

$$|\Delta_{-1}| = |\Delta_1|, \quad \Delta_0 = \sqrt{2}|\Delta_1|. \tag{2.10}$$

The other state denoted by SF_1 is described by $\vec{\Delta}_{\mathrm{fm}} = (\Delta_{-1}, 0, 0)$ or $\vec{\Delta}_{\mathrm{fm}} = (0, 0, \Delta_1)$: It breaks time-reversal symmetry, it is doubly degenerate and given the spin-triplet nature of the pairing it corresponds to an orbital ferromagnet [18,19]. It can be easily checked that the length of the vector $\vec{\Delta}$ is the same in both of these states. Furthermore, inclusion of the sixth order terms in the Ginzburg-Landau expansion lead to the same result: The states SF_0 and SF_1 will have the same free energy below T_c since the system gains exactly the same amount of energy condensing into one of these states. Also note that the accidental degeneracy between these two states implies that the corresponding chemical potentials will also be the same.

The multicomponent nature of the spin-triplet ($m_s = 0$) p-wave superfluid furnishes other possible solutions which have somewhat higher energy than $\mathcal{F}_{\min}$. For our subsequent discussion it is useful to briefly mention these states here. There are two particular order parameter configurations corresponding to the partially condensed states: The first state which we denote as SP_2 is defined by ($\Delta_0 = \sqrt{2/3}|\Delta_{\mathrm{fm}}|, \Delta_1 = \Delta_{-1}^* = 0$), while the second one SP_3 corresponds to ($\Delta_0 = 0, \Delta_{\pm 1} \neq 0$) with $|\Delta_{\pm 1}| = \sqrt{1/3}|\Delta_{\mathrm{fm}}|$. As it turns out, both of these states at $T \sim T_c$ have the same energy $\mathcal{F}_{\mathrm{opm}} = -100a^2/27b = 2\mathcal{F}_{\min}/3$. In what follows, we will use the insights from the spatially homogeneous Ginzburg-Landau theory to analyze the ground state properties in the presence of trapping potential. We will be mainly interested in finding out whether the ground state energy configuration changes with distance from the center of the trap. In particular, the phase relation (2.9) becomes useful in identifying the order parameter configurations with the lowest energy.

B. Self-consistency equations in the local density approximation

We include the effects of the trapping potential $V(\mathbf{r})$ using the local density approximation (LDA) [24]. LDA is valid when the size of the pairing gap greatly exceeds the single particle level spacing at the Fermi level [25]. Within the LDA scheme, the gradient terms of the density and pairing amplitude are neglected, so that one can adopt the Thomas-Fermi theory to describe the superfluid pairing. In principle, the corrections to the ground states due to the gradient terms can be found by perturbation theory [26].

We consider the trapping potential of the form $V(\mathbf{r}) = \sum_i \beta_i r_i^2/2$. Formally, the LDA is implemented by considering the nonlocal chemical potential

$$\mu(\mathbf{r}) = \mu - V(\mathbf{r}). \tag{2.11}$$

One could define center potential to be μ/μ_0. Then, the Fermi energy is related to the particle number by $\varepsilon_F = (3N\sqrt{\beta_x\beta_y\beta_z})^{1/3}/\sqrt{m}$ and the particles occupy the volume with length $R_i = \sqrt{2\varepsilon_F/\beta_i}$ which is the Thomas-Fermi radius in the ith direction. We can now express the harmonic trap in the unit of ε_F in the standard dimensionless form as $V(\mathbf{r})/\varepsilon_F = \sum_i (r_i/R_i)^2$ as given in Ref. [27]. Given (2.11) it follows that the order parameter components (2.4) and the particle density (2.5) depend on the position relative to the center of the trap, $\Delta_m \to \Delta_m(\mathbf{r})$, $n \to n(\mathbf{r})$. The total particle number in a trap is fixed, so in order to determine the global chemical potential μ, Eq. (2.11), we need to integrate both parts of the equation for $n(\mathbf{r})$ over the trap and normalize the resulting integrals by the volume of the trap. Since $n(\mathbf{r})$ depends on $\Delta_m(\mathbf{r})$, at each step of the calculation the self-consistency equations for $\Delta_m(\mathbf{r})$ must be solved. Note that unlike the case of the single channel model, the effective coupling constant $\lambda_{\text{eff}}(\mathbf{r}) = g^2/(\omega - 2\mu(\mathbf{r}))$ becomes dependent on the distance from the center of the trap and the population imbalance.

After the global chemical potential is found, we determine the spatial profile of the order parameter components $\Delta_m(\mathbf{r})$ allowing for all possible configurations as we have discussed above. At zero temperature, the ground state configuration at each point of the trap can be identified by computing the local energy

$$E_{\text{gs}} = \sum_{\mathbf{k}} [\xi_{\mathbf{k}} - E_{\mathbf{k}} + (E_{\mathbf{k}} - h)\cdot\theta(h - E_{\mathbf{k}})] + \sum_{m=-1}^{1} \frac{(\omega - 2\mu)}{g^2}|\Delta_m|^2, \tag{2.12}$$

where we have omitted the dependence on $\mathbf{r}$ for brevity. Lastly, we note that to describe the population imbalance we will work with the parameter h rather than the parameter $P = (N_\uparrow - N_\downarrow)/(N_\uparrow + N_\downarrow)$ for convenience. However, we will quote both values (h, P) where necessary.

III. PHASE DIAGRAM FOR TWO-CHANNEL MODEL

In this section we summarize our results for the two-channel case. But, first, we provide a few comments on the procedure we have used. In order to compute the dependence of the pairing amplitude on the distance from the center of a trap, we need to compute the global chemical potential (chemical potential at trap's center) from the particle number equation $N = \int d^3\mathbf{r}[n_\uparrow(\mathbf{r}) + n_\downarrow(\mathbf{r})]$ normalized by the volume of the trap, and the expression under the integral is given by the right hand side of the equation (2.5); the integration should be performed over the trap volume. While the global chemical potential is being determined we solve the self-consistency equations (2.4) taking into account (2.11) and the dependence of the effective coupling on $\mathbf{r}$. Note that due to the fact that the chemical potential at the trap's center is unique for all fermions across the trap; this guarantees that the only superfluid state which is realized in the trap in the SF_1 state since it will always have the lowest energy among all possible pairing states. This is in sharp contrast with the case of no trapping potential when for a given population imbalance, each pairing state has its

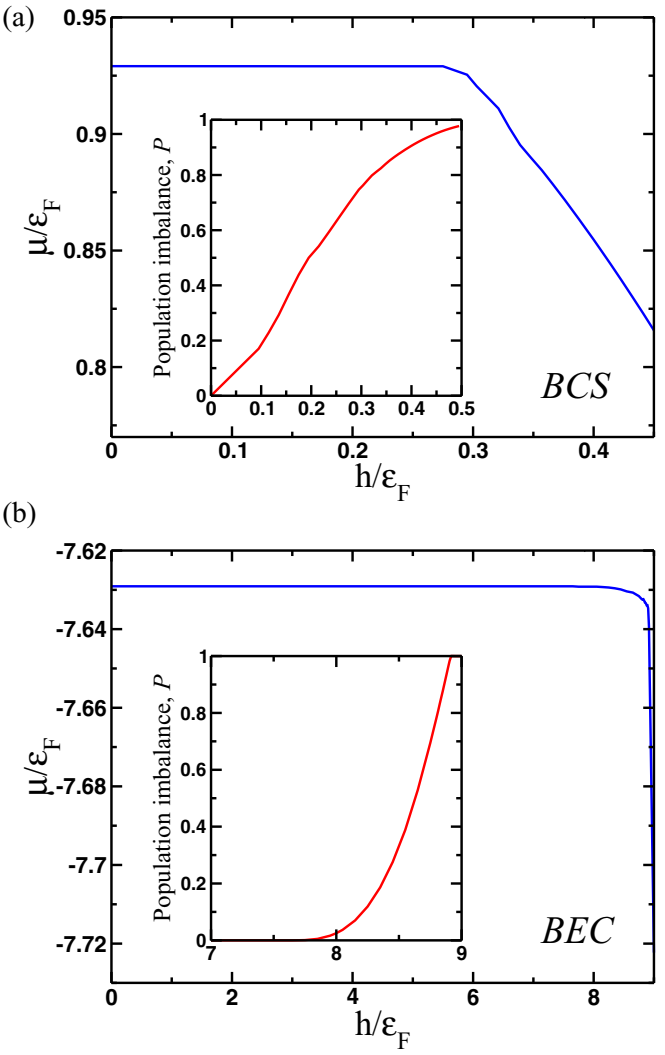

FIG. 2. Chemical potential and population imbalance (inset) as a function of parameter h (in the units of Fermi energy ε_F) calculated by solving the system of self-consistency and the particle number equations for harmonic trapping potential. The results are shown for the following choice of parameters: $\gamma = 1.45$, $n = 0.875$, while the detuning frequency is $\omega = 2\mu_0 + g^2\nu_F/3.15$ (BCS, top panel) and $\omega = 2\mu_0 + g^2\nu_F/5.96$ (BEC, bottom panel), where μ_0 is a chemical potential for $h = 0$.

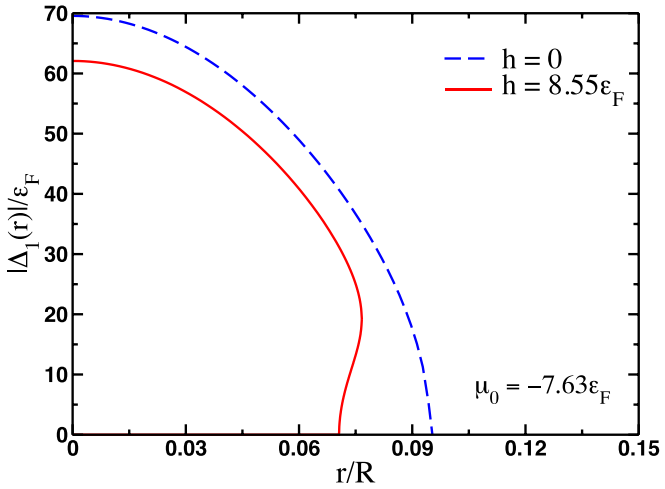

FIG. 3. Radial dependence of the pairing amplitude $|\Delta_1(r)|$ (SF_1) for zero and finite values of the parameter h (in the units of Fermi energy ε_F) calculated by solving the system of self-consistency and the particle number equations for a harmonic trapping potential. The results are shown for the following choice of parameters: $\gamma = 1.45$, $n = 0.875$, while the detuning frequency is $\omega = 2\mu_0 + g^2\nu_F/5.96$.

own chemical potential and the ground state is determined by comparing the energies of the corresponding superfluid states.

In Fig. 2 we show the results for the dependence of the global chemical potential μ, Eq. (2.11), on the parameter h, Eq. (2.2), for the superfluid states SF_1. As we have mentioned above, the nontrivial feature of the two-channel model is that the effective pairing strength depends on both population imbalance and trapping potential via its dependence on the chemical potential. Moreover, the difference in the values of the global chemical potential appears to be the main reason for the deviations from the ground and metastable energy configurations predicted by the Ginzburg-Landau expansion. We define our $(r/R)^2 = \sum_i (r_i/R_i)^2$ to account for any general harmonic trap throughout our one and two-channel results.

A. BEC regime

In Fig. 3 we show the radial dependence of the pairing amplitudes on the far BEC side of the FR. As one can see, at higher values of the population imbalance the pairing amplitude shows nonlinear dependence on r. This nonlinearity signals an instability of the spatially homogeneous solution at given r. Specifically, it suggests that if the size of the optical trap is large enough, the Cooper pairs will acquire some finite center-of-mass momentum forming a spatially inhomogeneous superfluid since the energy of this state becomes lower than the energy of the spatially homogeneous one. In conventional superconductors this state has been dubbed in literature as the Fulde-Ferrel-Larkin-Ovchinnikov (FFLO) state.

The phase diagram in the BEC regime is shown in Fig. 4(a). At low values of the population imbalance and close to the center of the trap the superfluid remains unpolarized and the single particle excitation spectrum remains gapped for all values of momenta. As one increases the value of the population imbalance, the system develops local polarization,

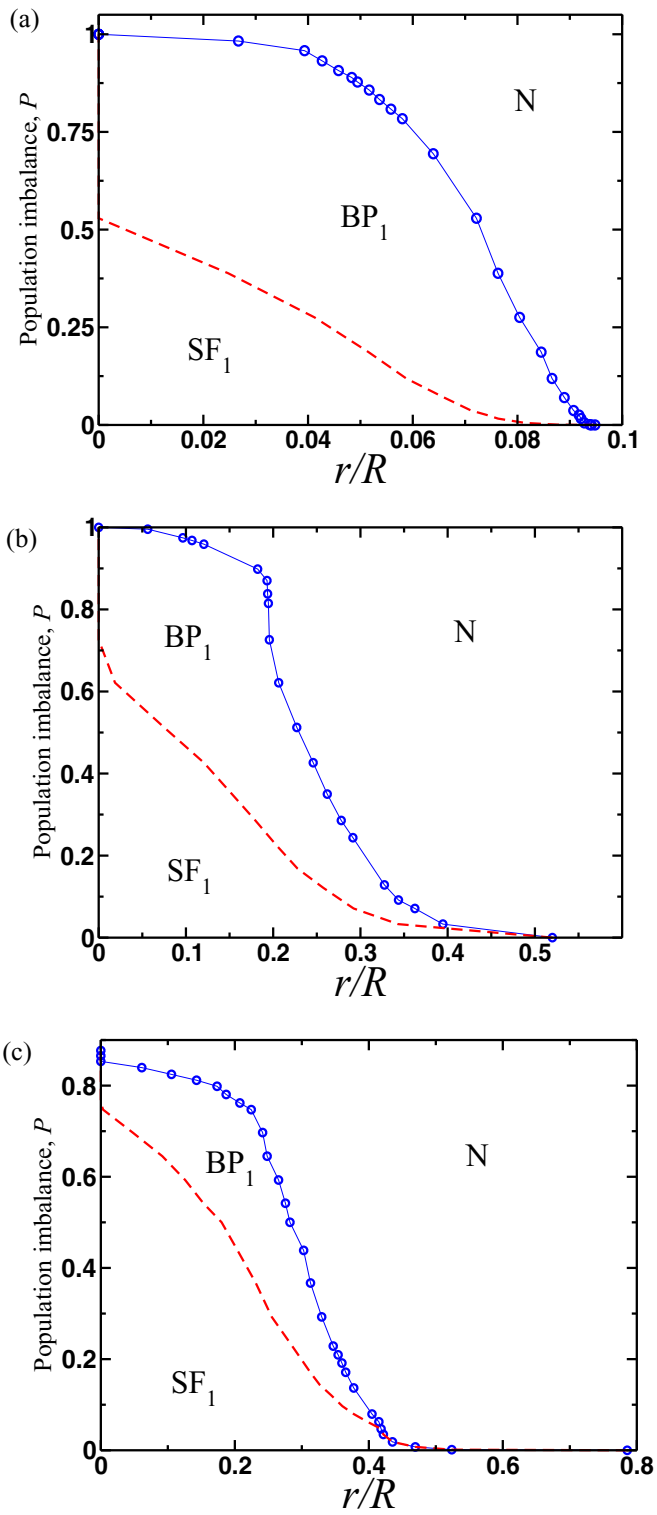

FIG. 4. Phase diagram for the BEC (top panel), crossover (middle panel), and BCS (bottom panel) regions in the (r, P) plane extracted from the data for the ground state energy density as a function of the distance from the center of the trap. The detuning frequencies are $\omega = 2\mu_0 + g^2\nu_F/2.35$ for the BCS region, $\omega = 2\mu_0 + g^2\nu_F/3.17$ for the crossover region, and $\omega = 2\mu_0 + g^2\nu_F/5.95$ for the BEC regions of the FR.

$n_\uparrow(\mathbf{r}) - n_\downarrow(\mathbf{r}) \neq 0$, which also corresponds to the emergence of the gapless excitations in given momentum interval where

$\sqrt{\xi_{\mathbf{k}}^2 + |\Delta(\hat{\mathbf{k}})|^2} - h \leqslant 0$. We call this state a breached paired state (BP_1) [27,28] and the dashed line separates unpolarized SF_1 and BP_1 states.

B. Crossover and BCS regimes

We carried out the calculation similar to the one above for the case when the detuning frequency is at close to the crossover regime so that the corresponding chemical potential is close to zero. We show the plot of the phase diagram on Fig. 4(b). The only quantitative difference with the BEC case is the narrowing of the region of the breach-pairing state. Lastly, the phase diagram in the BCS regime, Fig. 4(c) is again qualitatively similar to the diagram for two other regimes. Lastly, we note that unlike the BEC case, in BCS and crossover regimes, the superfluid state extends significantly far from the center of the trap. Part of the reason why this is observed in the one-channel model is that in two channels Δ remains unchanged as you go deep into BEC due to an extra term in the particle number equation.

IV. PHASE DIAGRAM FOR ONE-CHANNEL MODEL

In this section we present a summary of the results for the one-channel model. As we have emphasized above there are two main differences here compared to the two-channel model: (1) the coupling constant remains independent of the position in the trap and (2) the particle number equation does not have the term proportional to $|\Delta|^2/\lambda$, i.e., the first term on the right-hand side of equation (2.5). Therefore, in one-channel model the self-consistency and the number equations take the following form

$$\Delta_m = \lambda \sum_{E_{\mathbf{k}} \geqslant h} \frac{w_k^2}{2E_{\mathbf{k}}} \sum_{n=-1}^{1} Y_{1m}^*(\hat{\mathbf{k}}) Y_{1n}(\hat{\mathbf{k}}) \Delta_n,$$
$$2n = \sum_{\mathbf{k}} \left[1 - \frac{\xi_{\mathbf{k}}}{E_{\mathbf{k}}} \theta(E_{\mathbf{k}} - h)\right]. \tag{4.1}$$

Just as in the case of the two-channel model we have $n = (n_\uparrow + n_\downarrow)/2$, and the gap amplitudes and particle densities are functions of trap coordinates. We can also identically obtain the above equation by using the method of Green's function and deploying Matsubara's summations. In local density approximation (LDA), it is easy to show that the total particle number can be re-written as

$$1 = \frac{3}{\pi^3} \int d^3\tilde{r} \int d^3\tilde{\mathbf{k}} \left[1 - \frac{\xi_{\tilde{\mathbf{k}}}}{E_{\tilde{\mathbf{k}}}} \theta(E_{\tilde{\mathbf{k}}} - h)\right], \tag{4.2}$$

where $\tilde{r} = r/R$, $\tilde{k} = k/k_F$ while the gap components and single particle energies are normalized by the Fermi energy E_F. Lastly, in the local density approximation, population imbalance P can be computed according to the following equation

$$P = \frac{3}{\pi^3} \int d^3\tilde{r} \int d^3\tilde{\mathbf{k}} \theta(h - E_{\tilde{\mathbf{k}}}). \tag{4.3}$$

The chemical potential at any distance from trap center is given as $\mu(\tilde{r}) = \mu = \mu_0 - \tilde{r}^2$ in the units of Fermi energy E_F [27].

The free energy in the one-channel model takes the following form

$$E_{\text{gs}} = \sum_{\mathbf{k}} [\xi_{\mathbf{k}} - E_{\mathbf{k}} + (E_{\mathbf{k}} - h) \cdot \theta(h - E_{\mathbf{k}})] + \sum_{m=-1}^{1} \frac{|\Delta_m|^2}{\lambda}. \tag{4.4}$$

We present phase diagrams for both the BCS and BEC side of Feshbach resonance along with the local densities profiles. While solving for μ_0, i.e., the chemical potential at the trap's center, we make sure that we only accept lowest energy state pairing (SF_1) if its free energy Eq. (4.4) is less than the unpaired state at any distance from trap center. While solving for μ_0, the Ginzburg-Landau expansion dictates that lowest energy pairing state is the orbital ferromagnet. We then generate a phase diagram in the (r, P) plane by computing local polarization density. We also present some density

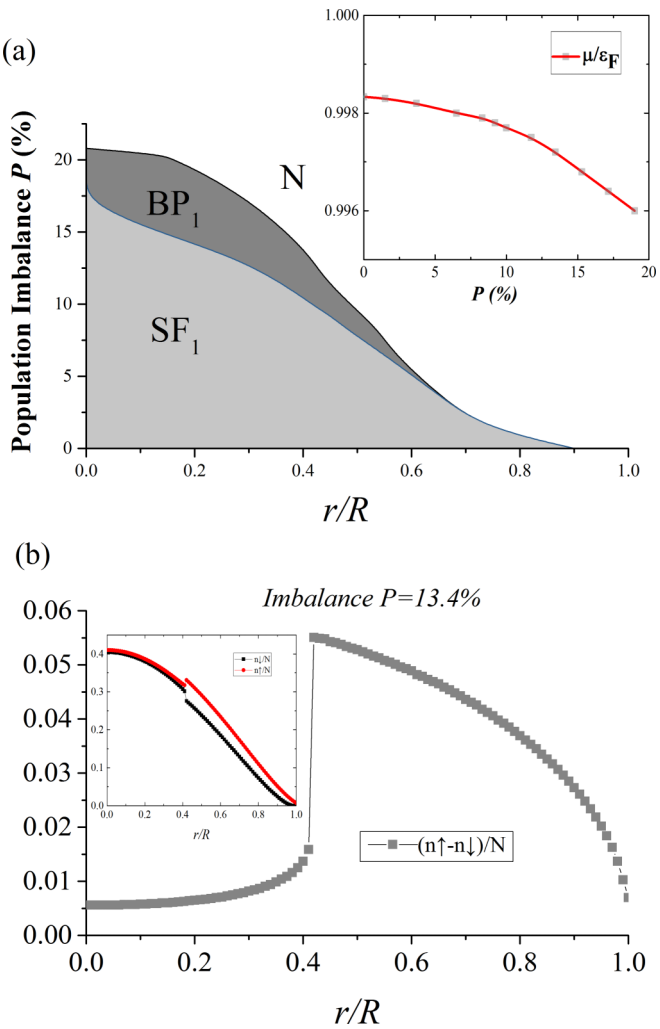

FIG. 5. (a) Phase diagram for the BCS region in the (r, P) plane extracted from the data for the ground state energy density as a function of the distance from the center of the trap. Inset is μ_0 as a function of imbalance. (b) Local spin/population densities and its ratio with local total number. The coupling constant is $\lambda = 1.45$.

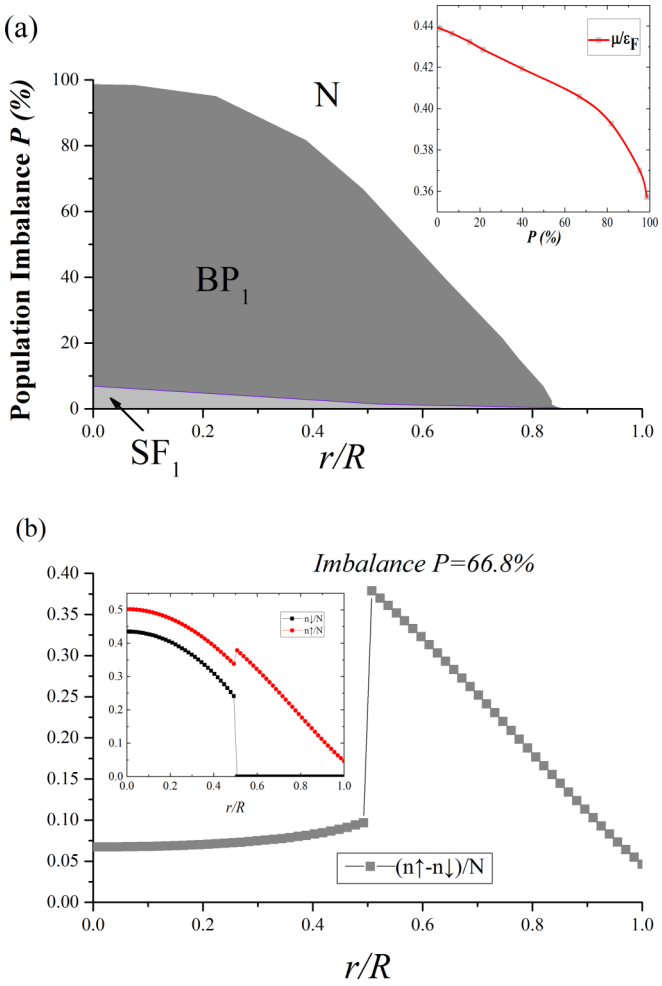

FIG. 6. (a) Phase diagram for the crossover region in the (r, P) plane extracted from the data for the ground state energy density as a function of the distance from the center of the trap. Inset is μ as a function of imbalance. (b) Local spin/population densities and its ratio with local total number. The coupling constant is $\lambda = 2.9$.

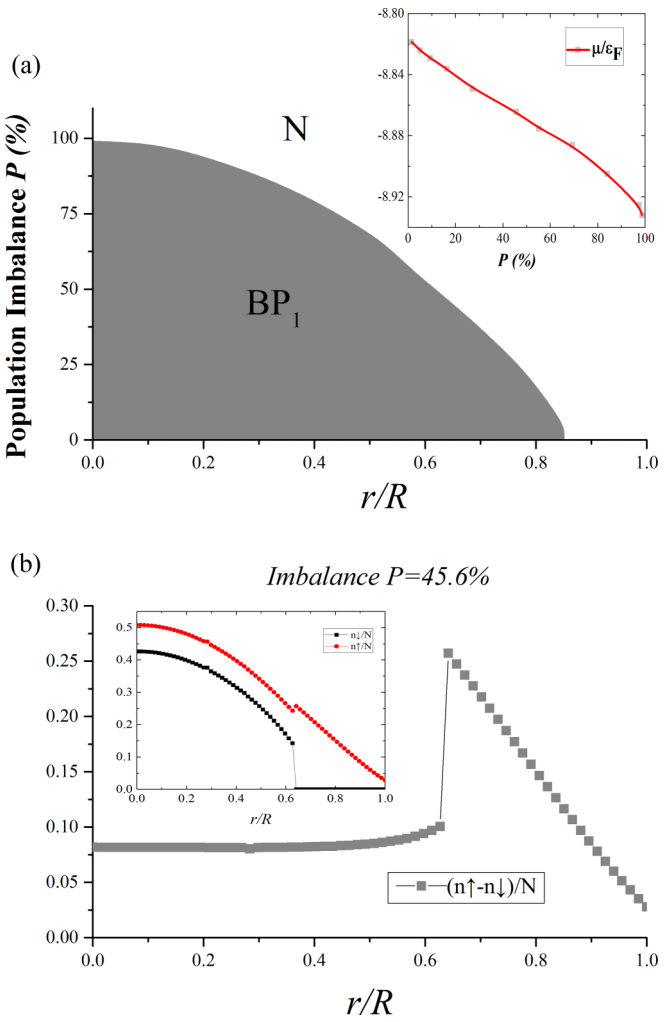

FIG. 7. (a) Phase diagram for the BEC region in the (r, P) plane extracted from the data for the ground state energy density as a function of the distance from the center of the trap. Inset is μ as a function of imbalance. (b) Local spin/population densities and its ratio with local total number. The coupling constant is $\lambda = 5.95$.

profiles for certain polarization at the BEC and BCS side of FR.

A. BCS regime

In Fig. 5 we present a phase diagram for the BCS side of the FR based on consideration of the lowest free energy pairing state SF_1. We find that as we increase population imbalance, superfluid core decreases its radius analogous to the s-wave case. The superfluid remains unpolarized at the trap center until imbalance is increased to about 18%. We also show that for finite population imbalance our system goes from SF_1/BP_1 state to normal state (N) through first order phase transition as can be seen from finite jump in $n_\uparrow - n_\downarrow$. The inset in Fig. 5(a) shows the dependence of μ_0 (in SF_1 state) on the population imbalance. We define our breached pair state BP_1 analogous to the two-channel model where $(n_\uparrow(\mathbf{r}) - n_\downarrow(\mathbf{r}))/(n_\uparrow(\mathbf{r}) + n_\downarrow(\mathbf{r})) \neq 0$, which also corresponds to the emergence of the gapless excitations in a given momentum interval where $\sqrt{\xi_{\mathbf{k}}^2 + |\Delta(\hat{\mathbf{k}})|^2} - h \leqslant 0$.

B. Crossover regime

In the crossover regime we present the phase diagram showing essentially the trend in between the BEC and BCS side. We have both SF_1 as well as BP_1 phases present up to finite population imbalance. At higher imbalances we have only the BP_1 state analogous to the BEC side which is present up to quite high population imbalances. From Fig. 6(b), we can see that the phase transition between BP_1 and normal state is first order in nature for high population imbalances. In the inset in Fig. 6(a) we plot the dependence of chemical potential at the trap's center against population imbalance.

C. BEC regime

As one can see from Fig. 7 on the BEC side of FR we find that the superfluid core exists only in the form of BP_1 and extends to much larger population imbalance compared to the BCS side. There is still the first order phase transition to the normal state for high population imbalance as shown in Fig. 7.

We also show in the inset the dependence of chemical potential at the trap's center on population imbalance.

To summarize, in this section we have shown that under LDA the p-wave superfluid is energetically favorable and exists as a core at the trap's center, analogous to the s-wave case. The superfluid exists in superfluid orbital ferromagnet state (SF_1) or breached pair state (BP_1). The normal state remains polarized as seen from the particle density plots. Finally, the radius of the superfluid core decreases with increasing polarization and at certain polarization the superfluid core disappears as it is not energetically favorable anymore.

V. CONCLUSIONS

In this paper we have studied the problem of the $m_s = 0$ triplet p-wave pairing for an atomic Fermi gas subject to a harmonic trapping potential within the mean-field approach. We presented the phase diagrams for both two- and one-channel pairing models. In particular, the mean-field results of the one-channel model are relevant for sufficiently wide resonances and away from the exact unitarity limit. We found that (i) as would be expected for a rotationally invariant case, the trapping potential does not affect the degeneracy between the superfluid state SF_0 with all nonzero angular momentum components of $\vec{\Delta}$ and the time-reversal symmetry broken state SF_1 when only one component of $\vec{\Delta}$ with either $m = 1$ or $m = -1$ is nonzero (so-called orbital ferromagnet); (ii) perhaps a somewhat less expected result is that close to the center of the trap, the time-reversal-breaking doubly degenerate superfluid state SF_1 which also has the same energy as SF_0 remains the ground state for any value of the population imbalance until the normal state becomes more energetically favorable.

ACKNOWLEDGMENTS

The authors express their gratitude to Prof. Emil Yuzbashyan for bringing this problem to their attention and related discussion. The authors also thank Anthony Leggett, Jason Ho, and Leo Radzihovsky for useful discussions. The work of A.K. and M.D. was financially supported by the National Science Foundation Grant No. DMR-1506547. M.D. thanks DAAD grant from German Academic Exchange Services for the partial financial support and Karlsruhe Institute of Technology, where part of this work has been completed, for hospitality.

APPENDIX: PROPERTIES OF THE SELF-CONSISTENCY EQUATIONS

The self-consistency equations (2.4) have a fairly complicated structure which significantly complicates their numerical analysis. With the help of the Ginzburgh-Landau expansion, we were able to demonstrate that only a few roots will give the minimum value for the free energy provided that the relation (2.9) is satisfied. Here, we show that the self-consistency equations have other nontrivial solutions for which the phase relation (2.9) holds. Thus, in our subsequent discussion we will only be interested in a superfluid state when all the angular momentum components of the pairing wave function are nonzero.

Let us re-write the self-consistency equations in a compact matrix form as follows

$$\Delta_m = \sum_{n=-1}^{1} \mathcal{K}_{mn}[\Delta] \cdot \Delta_n. \tag{A1}$$

The properties of the spherical components entering into (2.4) dictate $\mathcal{K}_{-1,1} = \mathcal{K}^*_{1,-1} \equiv |\mathcal{K}_1| e^{i\psi}$ and $\mathcal{K}_{0,1} = -\mathcal{K}_{-1,0} = |\mathcal{K}_{01}| e^{i\alpha}$. The diagonal components are purely real and we will use the following notations $\mathcal{K}_{-1,-1} = \mathcal{K}_{1,1} = \mathcal{K}_d$, $\mathcal{K}_{00} = \mathcal{K}_0$. As a result, adopting these notations, we cast the system of equations (2.4) into the following form:

$$\begin{aligned}
1 &= \mathcal{K}_d - |\mathcal{K}_{01}| \frac{\Delta_0}{|\Delta_{-1}|} e^{i(\alpha-\phi_{-1})} \\
&\quad + |\mathcal{K}_1| \frac{|\Delta_1|}{|\Delta_{-1}|} e^{i(\psi+\phi_1-\phi_{-1})}, \\
1 &= \mathcal{K}_0 - |\mathcal{K}_{01}| \frac{|\Delta_{-1}|}{\Delta_0} e^{-i(\alpha-\phi_{-1})} \\
&\quad + |\mathcal{K}_{01}| \frac{|\Delta_1|}{\Delta_0} e^{i(\alpha+\phi_1)}, \\
1 &= \mathcal{K}_d + |\mathcal{K}_{01}| \frac{\Delta_0}{|\Delta_1|} e^{-i(\alpha+\phi_1)} \\
&\quad + |\mathcal{K}_1| \frac{|\Delta_{-1}|}{|\Delta_1|} e^{-i(\psi+\phi_1-\phi_{-1})}
\end{aligned} \tag{A2}$$

and we take into account that the phases of the components $\Delta_{\pm 1}$ can always be taken relative to the phase of Δ_0, so that the latter is considered to be purely real. We have to keep in mind that all the matrix elements are the functions of Δ_0 and $\Delta_{\pm 1}$. Clearly two out of six of these equations are redundant since we have only five unknowns.

Let us take an imaginary part from the first and the third equations (A2) which yields

$$\begin{aligned}
|\mathcal{K}_{01}| \Delta_0 \sin(\alpha - \phi_{-1}) &= |\mathcal{K}_1| b \sin(\psi + \phi_1 - \phi_{-1}), \\
|\mathcal{K}_{01}| \Delta_0 \sin(\alpha + \phi_1) &= -|\mathcal{K}_1| a \sin(\psi + \phi_1 - \phi_{-1}).
\end{aligned} \tag{A3}$$

As we have seen from the Ginzburg-Landau analysis, the minimum of the free energy is achieved when (2.9) holds implying $\phi_1 = -\phi_{-1}$. Then there are two possible scenarios, which we would like to discuss separately.

1. Symmetric solution: $|\Delta_{-1}| = |\Delta_1|$

In the first one, one needs to require $|\mathcal{K}_{01}| = 0$ and $\phi_{-1} = \psi/2$. In turn, equation

$$|\mathcal{K}_{01}(\Delta_{-1}, \Delta_1, \Delta_0)| = 0$$

can only be satisfied for $|\Delta_{-1}| = |\Delta_1|$. Clearly, this solution corresponds to the fully condensed superfluid in a state with a global minimum of free energy. Furthermore, from the first equation (A2) it also follows that

$$\psi + 2\phi_1 = \pi n, \tag{A4}$$

where n is an integer, so that the phase of Δ_1 is basically determined by the phase of the off-diagonal matrix element

$\mathcal{K}_{-1,1}$. Furthermore, there are two roots corresponding to the even or odd values of n and one needs to compute the free energy to determine which of the two roots correspond to the ground state.

2. Asymmetric solution: $|\Delta_{-1}| \neq |\Delta_1|$

In the second scenario we impose the constraint on the nonvanishing K_{01} in (A3) so that from (A3) it follows that the following equation must be fulfilled:

$$|\Delta_{-1}|\sin(\alpha-\phi_{-1}) = -|\Delta_1|\sin(\alpha+\phi_1), \tag{A5}$$

which is the imaginary part of the second equation (A2). We still need to search for all possible solutions when $\phi_{-1} = -\phi_1$ since this relation guarantees the minimum in the free energy as we have seen from the Ginzburgh-Landau analysis. Then it immediately follows that equation (A5) has the following nontrivial solution

$$\alpha - \phi_{-1} = \pi n, \tag{A6}$$

where $n = 0,1,2,....$ Furthermore, since in this scenario $|\Delta_{-1}| \neq |\Delta_1|$ from the first two equations we can also obtain the following relation between the order parameter amplitudes:

$$\Delta_0^2 = (|\Delta_1| - |\Delta_{-1}|)^2\left(\frac{1-\mathcal{K}_d}{1-\mathcal{K}_0}\right). \tag{A7}$$

Thus, as we have seen there are two possible solutions corresponding to the fully condensed state. However, as we have checked by the direct numerical calculation, the state with $|\Delta_{-1}| \neq |\Delta_1|$ does not have energy lower than the state with $|\Delta_{-1}| = |\Delta_1|$ in agreement with the Ginzburg-Landau analysis.

[1] C. A. Regal, C. Ticknor, J. L. Bohn, and D. S. Jin, Phys. Rev. Lett. **90**, 053201 (2003).

[2] J. Zhang, E. G. M. van Kempen, T. Bourdel, L. Khaykovich, J. Cubizolles, F. Chevy, M. Teichmann, L. Tarruell, S. J. J. M. F. Kokkelmans, and C. Salomon, Phys. Rev. A **70**, 030702(R) (2004).

[3] C. Ticknor, C. A. Regal, D. S. Jin, and J. L. Bohn, Phys. Rev. A **69**, 042712 (2004).

[4] C. H. Schunck, M. W. Zwierlein, C. A. Stan, S. M. F. Raupach, W. Ketterle, A. Simoni, E. Tiesinga, C. J. Williams, and P. S. Julienne, Phys. Rev. A **71**, 045601 (2005).

[5] S. Saha, A. Rakshit, D. Chakraborty, A. Pal, and B. Deb, Phys. Rev. A **90**, 012701 (2014).

[6] V. Gurarie and L. Radzihovsky, Ann. Phys. **322**, 2 (2007), January Special Issue 2007.

[7] N. Read and D. Green, Phys. Rev. B **61**, 10267 (2000).

[8] V. Gurarie, L. Radzihovsky, and A. V. Andreev, Phys. Rev. Lett. **94**, 230403 (2005).

[9] M. S. Foster, V. Gurarie, M. Dzero, and E. A. Yuzbashyan, Phys. Rev. Lett. **113**, 076403 (2014).

[10] M. S. Foster, M. Dzero, V. Gurarie, and E. A. Yuzbashyan, Phys. Rev. B **88**, 104511 (2013).

[11] C.-Y. Lai, C. Shi, and S.-W. Tsai, Phys. Rev. B **87**, 075134 (2013).

[12] R. Casalbuoni and G. Nardulli, Rev. Mod. Phys. **76**, 263 (2004).

[13] W. A. Coniglio, L. E. Winter, K. Cho, C. C. Agosta, B. Fravel, and L. K. Montgomery, Phys. Rev. B **83**, 224507 (2011).

[14] A. Bulgac, M. M. Forbes, and A. Schwenk, Phys. Rev. Lett. **97**, 020402 (2006).

[15] W. Yi and L.-M. Duan, Phys. Rev. A **73**, 031604 (2006).

[16] G.-D. Lin, W. Yi, and L.-M. Duan, Phys. Rev. A **74**, 031604 (2006).

[17] W. Zhang and L.-M. Duan, Phys. Rev. A **76**, 042710 (2007).

[18] T.-L. Ho and R. B. Diener, Phys. Rev. Lett. **94**, 090402 (2005).

[19] R. Liao, F. Popescu, and K. Quader, Phys. Rev. B **88**, 134507 (2013).

[20] R. Liao, Ph.D. thesis, Kent State University (2008).

[21] S. S. Botelho and C. A. R. S. Melo, J. Low Temp. Phys. **140**, 409 (2005).

[22] P. Nozières and S. Schmitt-Rink, J. Low Temp. Phys. **59**, 195 (1985).

[23] E. A. Yuzbashyan, M. Dzero, V. Gurarie, and M. S. Foster, Phys. Rev. A **91**, 033628 (2015).

[24] C.-C. Chien, Q. Chen, Y. He, and K. Levin, Phys. Rev. Lett. **98**, 110404 (2007).

[25] S. Giorgini, L. P. Pitaevskii, and S. Stringari, Rev. Mod. Phys. **80**, 1215 (2008).

[26] A. Csordás, O. Almásy, and P. Szépfalusy, Phys. Rev. A **82**, 063609 (2010).

[27] W. Yi and L.-M. Duan, Phys. Rev. A **74**, 013610 (2006).

[28] W. Yi and L.-M. Duan, Phys. Rev. Lett. **97**, 120401 (2006).